
A Mouse Optical Simulation Environment (MOSE) to Investigate Bioluminescent Phenomena in the Living Mouse with the Monte Carlo Method¹

Hui Li, MS, Jie Tian, PhD, Fuping Zhu, PhD, Wenxiang Cong, PhD, Lihong V. Wang, PhD, Eric A. Hoffman, PhD, Ge Wang, PhD

Rationale and Objectives. As an important part of bioluminescence tomography, which is a newly developed optical imaging modality, mouse optical simulation environment (MOSE) is developed to simulate bioluminescent phenomena in the living mouse and to predict bioluminescent signals detectable outside the mouse. This simulator is dedicated to small animal optical imaging based on bioluminescence.

Materials and Methods. With the parameters of biological tissues, bioluminescent sources, and charge coupled device (CCD) detectors, the 2-dimensional/3-dimensional MOSE simulates the whole process of the light propagation in 2-dimensional/3-dimensional biological tissues using the Monte Carlo method. Both the implementation details and the software architecture are described in this article.

Results. The software system is implemented in the Visual C++ programming language with the OpenGL techniques and has a user-friendly interface facilitating interactions relevant to bioluminescent imaging. The accuracy of the system is verified by comparing the MOSE results with independent data from analytic solutions and commercial software.

Conclusion. As shown in our simulation and analysis, the MOSE is accurate, flexible, and efficient to simulate the photon propagation for bioluminescence tomography. With graduate refinements and enhancements, it is hoped that the MOSE will become a standard tool for bioluminescence tomography.

Key Words. Bioluminescent imaging; light propagation; biological tissues; Monte Carlo simulation.

© AUR, 2004

Small animal imaging using bioluminescent sources has become increasingly important over recent years. The use

of bioluminescent sources, such as cells tagged with light-emitting probes, allows in vivo detection of molecular and cellular events such as gene expression (1–3). The University of Iowa (Iowa City, IA), is developing an in vivo bioluminescence tomography system integrated with an X-ray computed tomography (CT)/micro-CT scanner (4,5). The novel concept is to collect emitted photons from multiple 3-dimensional (3D) directions with respect to a living mouse marked by bioluminescent reporter luciferases, and reconstruct an internal bioluminescent source distribution based on both outgoing bioluminescent signals and CT/micro-CT volume of the mouse. The 3D bioluminescent source distribution and corresponding CT/micro-CT volume are then registered.

Because an analytic solution to the radiative transport equation is extremely difficult to obtain in the practical situation, numerical simulation plays a critical role in the

Acad Radiol 2004; 11:1029–1038

¹ From the Medical Image Processing Group, Key Laboratory of Complex Systems and Intelligence Science, Institute of Automation, Chinese Academy of Science, Beijing, China (H.L., J.T., F.Z.); and the CT/Micro-CT Laboratory, Departments of Radiology & Biomedical Engineering, University of Iowa, Iowa City, IA, 52242 (W.C., E.A.H., G.W.); and the Optical Imaging Laboratory, Department of Biomedical Engineering, Texas A & M University, College Station, TX (L.V.W.). Received January 14, 2004; revision requested March 26; revision received May 2; accepted May 3. Supported in part by the National Institutes of Health grant no. R21/R33 EB001685, the National Science Fund for Distinguished Young Scholars of China under grant no. 60225008, and the Special Project of National Grand Fundamental Research 973 Program of China under grant no. 2002CCA03900. **Address correspondence to** G.W. University of Iowa, Iowa City, Iowa 52242; e-mail: WangG@mail.medicine.uiowa.edu; or J.T., Institute of Automation, Chinese Academy of Sciences, PO Box 2728, Beijing, 100080, China; e-mail: tian@doctor.com

© AUR, 2004

doi:10.1016/j.acra.2004.05.021

area of bioluminescence tomography. The Monte Carlo method is popular for simulation of light propagation in turbid biological tissues, because it is accurate, flexible, and can be readily accelerated using parallel processing techniques. Although a number of Monte Carlo programs for light transport simulation are available (6–12), they are either too general to be effective or are based on a geometric difference from that of the small animal of our primary interest. Furthermore, these programs do not allow various interventions and explorations we need for bioluminescent imaging.

In this article, we report our development of a mouse optical simulation environment (MOSE) using the Monte Carlo method to simulate the bioluminescent phenomena and predict bioluminescent signals outside the mouse in its spectral range. MOSE data were compared with independent analytic and numerical results to verify the accuracy of the MOSE.

MATERIALS AND METHODS

Nomenclature

Each biological tissue can be described by two sets of parameters: optical and geometric parameters. Four essential optical parameters are the refractive index n , the absorption coefficient μ_a (cm^{-1}), the scattering coefficient μ_s (cm^{-1}), and the anisotropy factor g (6). The total interaction coefficient μ_t is the sum of the absorption coefficient and the scattering coefficient. The anisotropy g is the average of the cosine value of the deflection angle (6). Geometric parameters include the coordinates and shapes of biological tissues. Each biological tissue can be composed of building blocks including ellipsoids, cylinders, polyhedrons, and so on. In addition to the Cartesian coordinate system, a moving spherical system was used with the same origin as that of the Cartesian system. The azimuthal angle ϕ and deflection angle θ are the two critical parameters in this spherical system.

There are additional parameters related to the simulation that describe the behaviors and properties during the photon transport process. The position of a photon packet is represented by Cartesian coordinates (x, y, z) . The direction of photon propagation is represented by the directional cosines (μ_x, μ_y, μ_z) . The energy of each photon packet is described by parameter w , whose incident value is the sum of light energy divided by the total number of photon packets. When photon packets travel from one site to another, the weight will be reduced. If the value of

weight is less than the given threshold, the photon packet will be subject to the Russian roulette technique. The step size s means the optical distance of a photon from the present location to the next interaction site.

Photon Propagation

The MOSE is designed to simulate the light transport in both 2-dimensional (2D) and 3D tissues. Building blocks include ellipses, rectangles, polygons, and so on in 2D cases; and ellipsoids, cylinders, polyhedrons, and so on in 3D cases. The bioluminescent sources include point, solid, and hollow sources constructed by building blocks as previously mentioned. Eventually, these building blocks will be extended into segmented regions. In the following article, our work focuses on the 3D MOSE for brevity.

Figure 1 is the flowchart for the whole simulation process. First, one photon packet is generated from a bioluminescent source distribution by positional and angular sampling. The photon packet then begins its transportation in biological tissues. It may be absorbed, scattered, internally reflected, and transmitted. A CCD camera will record the photon packet if it escapes from the mouse. The key in the Monte Carlo simulation is the sampling of a random variable from a probability distribution. Given a probability density function $p(x)$ in a interval (a, b) , we have

$$\int_a^x p(x') dx' = F(x) = \xi \quad \text{for } \xi \in (0, 1), x \in [a, b], \quad (1)$$

where ξ is a uniform unit random number (13–15). The random variable subject to $p(x)$ is obtained by solving equation 1 for x .

Photon generation.—In this work, we are mainly interested in point and solid sources. Generally speaking, both positional and angular sampling operations are needed to generate a photon packet based on the Monte Carlo method. Positional sampling finds the initial position of a photon packet, while angular sampling decides the direction of photon transportation. The photon generation in the current version of the MOSE is realized assuming a monotonic source uniformly distributed in its domain that can be readily generalized as needed.

Photon movement.—During the photon propagation, the key is to determine the next interaction site or the step size of the photon packet s , which is calculated as follows (6):

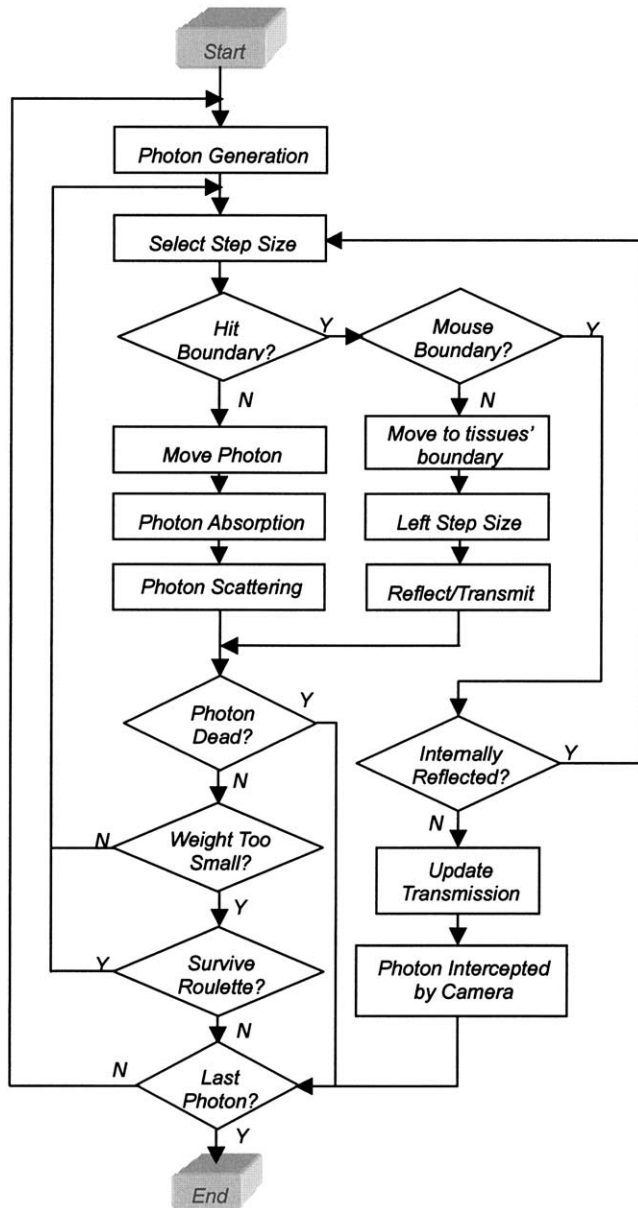


Figure 1. Flowchart of MOSE with the Monte Carlo method.

$$s = \frac{-\ln \xi}{\mu_a + \mu_s} = \frac{-\ln \xi}{\mu_t},$$

where ξ is a uniform random number in (0,1).

However, when the photon packet transports from the present interaction site to the next interaction site, it may hit the boundary of current tissue with adjoining tissues or the ambient medium. Therefore, we must first judge whether the photon packet hits a boundary with the calculated step of size s . Because each tissue is made up of

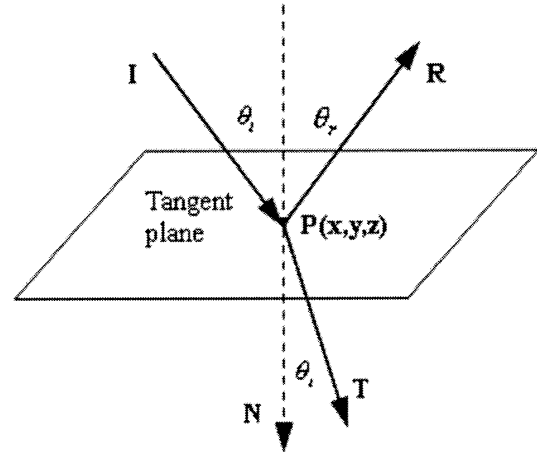


Figure 2. Geometry of photon internal reflection and photon transmission at the boundary of tissues. Unit vectors I, R, and T represent the direction vectors of incident photon, internally reflected photon, and transmitted photon, respectively. Vector N represents the outside normal direction of the tangent plane at point P(x, y, z). Angles $\theta_i, \theta_r, \theta_t$ represent the incident angle, internally reflected angle, and transmitted angle, respectively.

building blocks with known regular geometric shapes, it is straightforward to describe the current tissue where the photon packet is located and the neighboring tissues/medium where the next interaction may occur. If the photon propagation only involves one tissue, the photon packet will not hit the boundary. Then, s is the actual step size that photon packet will take. Otherwise, the step size (s) must be modified to the distance from the present interaction site to the photon exit point at the boundary.

Boundary effect.—Assume the current direction of a photon packet and the normal at a boundary point as unit vectors $U(\mu_x, \mu_y, \mu_z)$ and $N(\mu_x, \mu_y, \mu_z)$ respectively, the cosine of the incident angle $\cos\alpha_i$ is computed by the dot product of these two vectors. Then two important parameters critical angle $\alpha_{critical}$ and the internal reflectance $R(\alpha_i)$ must be calculated. Merely related with refractive indices of media n_i and n_t which a photon package is incident from and transmitted to respectively, the critical angle $\alpha_{critical}$ can be calculated (6,13). $R(\alpha_i)$ is determined by Fresnel's formulas (16):

$$R(\alpha_i) = \frac{1}{2} \left[\frac{\sin^2(\alpha_i - \alpha_t)}{\sin^2(\alpha_i + \alpha_t)} + \frac{\tan^2(\alpha_i - \alpha_t)}{\tan^2(\alpha_i + \alpha_t)} \right],$$

where α_i is the angle of incidence, and α_t represents the angle of transmission. Finally, a random number of the uniform unit ξ is generated. If $\xi \leq R(\alpha_i)$, the photon

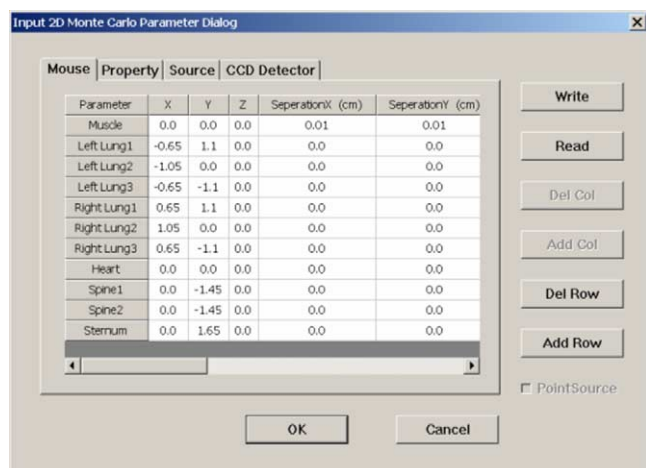


Figure 3. Input parameter dialog in MOSE.

packet is internally reflected by the boundary; otherwise it may be reflected or go across the boundary.

If the photon packet is internally reflected, the photon packet stays at the boundary and its directional cosine (μ_x, μ_y, μ_z) must be changed. As shown in Figure 2, incident directional cosines, internally reflected directional cosines, and the unit normal are denoted by unit vectors $I(\mu_x, \mu_y, \mu_z)$, $R(\mu'_x, \mu'_y, \mu'_z)$ and $N(\mu_{nx}, \mu_{ny}, \mu_{nz})$, respectively. Then $R(\mu'_x, \mu'_y, \mu'_z)$ can be calculated by $R = I - 2(I \cdot N)N$.

If the photon packet is transmitted from one region to another, the directional cosines of the photon packet are changed from $I(\mu_x, \mu_y, \mu_z)$ to $T(\mu_x^T, \mu_y^T, \mu_z^T)$. As shown in Figure 2, it can be verified that

$$T = \sin \theta_i \cdot \frac{I - (I \cdot N)N}{|I - (I \cdot N)N|} + \text{SIGN}(I \cdot N) \cdot \cos \theta_i \cdot N,$$

the photon weight is then added into the transmission matrix.

Photon absorption.—When a photon reaches the new interaction site, its energy or weight must be reduced, ie, the photon is partly absorbed while reaching the interaction site. Initially, a unit (or prespecified) weight is assigned to a photon package. After each propagation step, the photon packet is split into absorbed and scattered parts respectively. The weight of the absorbed fraction is stored into an absorption matrix, the photon weight is then updated by $w^t = aw$ for scattering, where a is the single particle albedo.

Photon scattering.—Once a photon package reaches a new site, not only its weight but also its travel direction

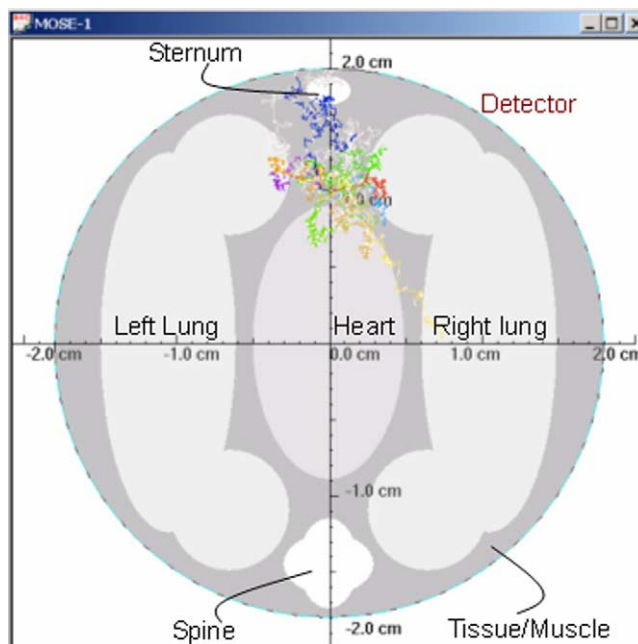


Figure 4. Paths of photon propagations in mouse chest phantom.

should be changed. That is, the azimuthal angle ϕ and deflection angles θ must be appropriately modified. Specifically, the probability function of the azimuthal angle ϕ is uniformly distributed over the interval $(0, 2\pi)$. The probability function of $\cos\theta$ is described by the Henyey-Greenstein function (17). With the Monte Carlo sampling, it is easy to calculate the new direction of the photon packet by the transform between the moving spherical coordinates and the Cartesian ones.

Photon termination.—There are two ways for a photon packet to complete its propagation. That is, it may be totally absorbed by tissues or captured by a CCD camera. Russian roulette technique (18) is used to terminate a photon packet once its weight drops below a specified threshold (eg, 0.0001). This test gives the photon packet one chance in m (eg, $m = 10$) for surviving with an amplified weight according to the following rules:

$$w = \begin{cases} mw & \text{if } \xi \leq 1/m \\ 0 & \text{others} \end{cases},$$

where ξ is a uniform unit random number.

Software Description

Functions and interface.—The MOSE has many built-in simulation functions and a user-friendly interface

Table 1
Bioluminescent Source Parameters Used in Three Simulated Experiments

Experiment No.	Radius (mm)	Center (mm)	Total Flux (W)	Total Number of Photons	Angle Distribution
1	0.3	(0,0,0)	1	10^5	uniform
2	0.3	(0,0,0)	1	10^5	uniform
3	1.0	(0,0,0)	1	10^5	uniform

handling input parameters, output files, and display. In the MOSE, 2D and 3D simulation are enabled in the same program framework. The two modes can be switched by pressing a button on the interface.

The MOSE implements all the functions described in the above sections via a user-friendly interface created with the Visual C++ programming language and OpenGL techniques. With an input parameter dialogue box, the operator can conveniently pass information into the system from database files, and add, delete, and modify the parameters as needed. In general, the input parameters can be classified into four categories: geometrical parameters of the biological tissues, optical parameters of biological tissues, parameters of bioluminescent sources, and parameters of the CCD camera. As shown in Figure 3, four separate pages in the input dialogue box correspond to these four kinds of parameters, respectively. Given the 2D/3D input parameters, the 2D/3D picture of the mouse tissues can be seen in the graphical interface.

There are three choices for display of the photon propagation process in biological tissues: tracing all the photon propagation paths, only tracing those photons that reach detectors, and only tracing the photons with selected indexes. We can then observe the photon transport through the biological tissues in real-time. The transport paths of different photon packages are highlighted in different colors as shown in Figure 4. While tracing photon packets, the operator may stop and restart the display of tracing by pressing a switch button at any moment. Once

the simulation is finished, we can retrieve output files recording the absorption data, transmission data, detector data, running time, and so on. The distribution maps of absorption and transmission can be graphically displayed as needed.

In the 3D interface, we can perform common operations such as rotation, zoom in, and zoom out with the left and middle mouse buttons. In addition to the display of the 3D detector configuration, the 2D slice of the detector array (ie, each cross-section of the 3D detector configuration) can be displayed with respect to its longitudinal coordinate. When a pseudo color scheme is chosen, different values of absorption and detector data are presented in different colors. Hence, the distribution of escaped and absorbed photons can be visually appreciated. The user-friendly interface is constructed completely using OpenGL techniques.

Rough-to-fine search.—Given a point inside the mouse, it will be time-consuming to find the tissue that contains the point if there are many building blocks used to represent the mouse. A two-step strategy referred to as the “rough-to-fine search” method was used to speed up the process.

A rough search is performed. After the geometric parameters are input, we not only record the indexes of tissues but also generate two tables T_1 and T_2 , respectively. Table T_1 has the same size of a pre-specified underlying image matrix, and records all the indexes of the biological tissues as approximated by a minimum rectangle containing each building block. Table T_2 is a 2D symmetric

Table 2
Optical Parameters of Biological Tissues Used in Three Simulated Experiments

Experiment No.	Absorption Coefficient μ_a (mm^{-1})	Scattering Coefficient μ_s (mm^{-1})	Refractive Index (n)	Anisotropy Coefficient (g)
1	0.02	15	1.37	0.94
2	0.082	10.27	1.37	0.90
3	0.30	16	1.37	0.85

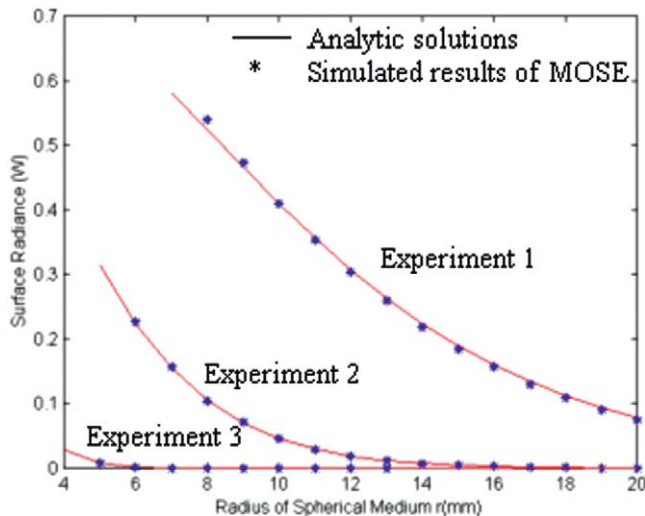


Figure 5. Three comparisons between analytical solutions of steady-state diffusion equation and simulated results of MOSE. In experiment 1, the radius of bioluminescent source R is 0.3 mm; the absorption coefficient μ_a is 0.02; the scattering coefficient μ_s is 15 mm⁻¹; the anisotropy coefficient g is 0.94 mm⁻¹. In experiment 2, R is 0.3 mm; μ_a is 0.082 mm⁻¹; μ_s is 10.27 mm⁻¹; g is 0.90. In experiment 3, R is 1.0 mm; μ_a is 0.30 mm⁻¹; μ_s is 16 mm⁻¹; g is 0.85. With different radii of spherical medium, the simulated results of MOSE are consistent with analytic solutions.

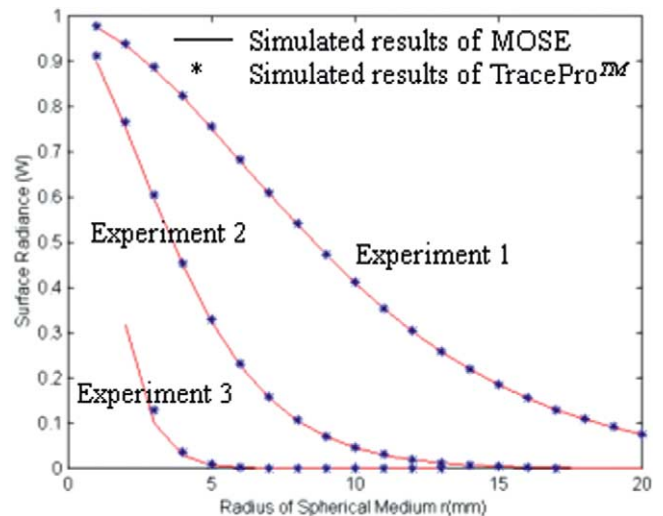


Figure 6. Three comparisons between simulated results of TracePro and those of MOSE. In experiment 1, the radius of bioluminescent source R is 0.3 mm; the absorption coefficient μ_a is 0.02; the scattering coefficient μ_s is 15 mm⁻¹; the anisotropy coefficient g is 0.94 mm⁻¹. In experiment 2, R is 0.3 mm; μ_a is 0.082 mm⁻¹; μ_s is 10.27 mm⁻¹; g is 0.90. In experiment 3, R is 1.0 mm; μ_a is 0.30 mm⁻¹; μ_s is 16 mm⁻¹; g is 0.85. It is easy to see that the simulated results of MOSE and TracePro are in accord with each other. The abscissa of the figure is the radius of the spherical medium; the Y-coordinate is the incident radiance on spherical surfaces with different radii.

matrix reflecting the intersecting relationship of these rectangles. If rectangles i and j overlap each other, the element $T_2(i,j)$ and $T_2(j,i)$ are set to 1; otherwise $T_2(i,j)$ and $T_2(j,i)$ are set to 0. Consequently, given a point (x,y,z) we can effectively reduce the index range to a limited number of building blocks, at least one of which contains the point.

Although the table search can be performed quickly, there are ambiguities on the boundaries and in the intersecting regions of building blocks. Therefore, a fine search is needed to either verify or modify the rough search result. Specifically, we compute the boundary function $F_k(x,y,z)$ of each building block one by one to find all k values such as $F_k(x,y,z) > 0$, where $k \in \{k | T_2(i,k) = 1\}$. Together with the “minimum area/volume” method introduced in the following section, the right tissue with a certain point can be located accurately.

Minimum area/volume.—In MOSE, when different tissues intersect each other, it is important to determine the boundary and optical parameters of the intersection. A method termed “minimum area/volume” is used in 2D/3D MOSE. Because each tissue is composed of building blocks with known regular geometry, we can search through the building blocks as mentioned above to determine intersecting blocks. The area/volume of each inter-

secting building block is then computed; the boundary and optical parameters of the intersecting block when given the minimum area/volume are used for simulation. In the experiments with 2D/3D MOSE, the program running time can be greatly reduced by the “minimum area/volume” criterion and the “rough-to-fine search” method.

RESULTS

The accuracy of the MOSE software system is verified in this section. Once the programs are validated, the statistical error inherent in Monte Carlo simulation can be estimated. With a large sample number (N), the relative error of the MOSE can be calculated by

$$R = \sqrt{\frac{\overline{x^2} - \bar{x}^2}{N}} / \bar{x}$$

where $\bar{x} = E(x) = \int xp(x)dx$ is the expected value of the random variable x , $\overline{x^2}$ is calculated by the formula $\overline{x^2} = \int x^2p(x)dx$, and $p(x)$ is the probability density function of the random variable x .

Table 3
Positional and Optical Parameters of Tissues in 2D Mouse Chest Phantom

Parameter	x [mm]	y [mm]	a [mm]	b [mm]	N[-]	Ua[/cm]	Us[/cm]	g[-]
Tissue/muscle	0.0	0.0	18.0	18.0	1.37	0.1	40	0.9
Left lung 1*	-6.5	1.1	4.0	4.0	1	3.5	230	0.94
Left lung 2*	-10.5	0.0	4.5	12.5	1	3.5	230	0.94
Left lung 3*	-6.5	-11.0	4.0	4.0	1	3.5	230	0.94
Right lung 1†	6.5	11.0	4.0	4.0	1	3.5	230	0.94
Right lung 2†	10.5	0.0	4.5	12.5	1	3.5	230	0.94
Right lung 3†	6.5	-11.0	4.0	4.0	1	3.5	230	0.94
Heart	0.0	0.0	5.0	9.0	1.37	2.0	160	0.85
Spine 1	0.0	-14.5	3.0	2.0	1.37	0.02	200	0.9
Spine 2	0.0	-14.5	2.0	3.0	1.37	0.02	200	0.9
Sternum	0.0	16.5	1.5	1.0	1.37	0.02	200	0.9

*The model of the left lung in mouse chest phantom is made up of three elliptic parts named as Left Lung 1, Left Lung 2, and Left Lung 3.

†The model of the right lung in mouse chest phantom is made up of three elliptic parts named as Right Lung 1, Right Lung 2, and Right Lung 3.

Comparison with the Analytic Solution

Approximately, the bioluminescent phenomena in biological tissues can be described by the steady-state diffusion equation (19). It is hard to find its analytic solution in most cases. However, with a solid spherical source and an infinite homogeneous medium, the analytic solution to the diffusion equation was recently obtained (19). To verify the accuracy of the MOSE, computer experiments were performed assuming a spherical solid source in an infinite homogeneous medium. The simulation parameters are listed in Tables 1 and 2, respectively. An excellent agreement was observed between the analytic results and the MOSE data as shown in Figure 5.

Comparison with the TracePro Data

TracePro (Lambda Research Corporation, Littleton, MA) is a commercial software system for simulation of light transport processes under various conditions. The Monte Carlo method is also used in this package (20). Three comparison experiments have been performed with the given spherical surface source in an infinite homogeneous medium and the simulation parameters shown in Tables 1 and 2. The incident radiances on various spherical detection surfaces of different radii were simulated by the MOSE and the TracePro, respectively. Figure 6 confirms that these two independently developed simulators produced very consistent data.

The comparison was then performed using a 2D/3D mouse chest phantom we designed for studies on bioluminescence tomography. The 3D version of the chest phan-

tom consists of cylinders forming left and right lungs, heart, spine, sternum, and background tissue, respectively. The 2D counterpart is a cross-section of the 3D phantom (as shown in Fig 4) where detectors are uniformly distributed in immediate contact with the mouse skin. All the optical parameters of 2D/3D mouse chest phantom are based on ex vivo data as summarized in Table 3.

Using 3D MOSE, 10 simulations were performed with a point source being located at (0, 1, 0). Each simulation contains 100,000 photon packets. In this case, the standard errors of the total absorption and total transmittance were 2.6805e-004 and 2.7662e-004, while the relative errors of these quantities were 1.3943e-003 and 3.5212e-004, respectively. The average running time was about 298 seconds. The 3D simulation results were then compared with that from the TracePro. With TracePro data as reference, the standard errors of the total absorption and total transmittance with the MOSE were 3.7237e-004 and 3.5326e-004, while the relative errors of these quantities were 2.0713e-003 and 4.3255e-004, respectively.

Comparison with Phantom Experimental Data

To verify MOSE, three experiments were designed and results were compared with phantom data. Parameters of bioluminescent sources, biological tissues, and CCD detectors are shown in Tables 4, 5, and 6, respectively.

In the first experiment, with a point source located at the center of the bottom plane and the rectangle CCD detector plane parallel to the top plane of a cylindrical tissue block (Fig 7), we obtained both experimental and

Table 4
Bioluminescent Source Parameters Used in Comparison Between MOSE and Three Phantom Studies

Experiment No.	Total Number of Sources	Shape	Center (mm)	Radius of Base (mm)	Height (mm)	Total Number of Photons	Total Flux (W/m ²)
1	1	cylinder	(0, 0, -5)	0.025	0.01	4.0e + 6	0.12
2	1	cylinder	(0, 0, 5.4)	1.5	0.01	1.0e + 7	0.12
3	2	cylinder	Source 1: (0, 0, 5.4) Source 2: (6, 0, 5.4)	1.5	0.01	1.0e + 7	0.025

Table 5
Biological Tissue Parameters Used in Comparison Between MOSE and Three Phantom Studies

Experiment No.	Center of Cylinder	Radius of Base (mm)	Height (mm)	Absorption Coefficient	Scattering Coefficient	Refractive Index	Anisotropy Coefficient
1	(0, 0, 0)	15.95	10	0.10 mm ⁻¹	3.0 mm ⁻¹	1.37	0.80
2	(0, 0, 0)	9.5	15	0.10 mm ⁻¹	3.0 mm ⁻¹	1.37	0.80
3	(0, 0, 0)	9.5	15	0.10 mm ⁻¹	3.0 mm ⁻¹	1.37	0.80

numerical transmission profiles on CCD detector plane as shown in Figure 8. These figures indicate that the transmission profile of MOSE is not as smooth as the experimental one because the photon number used in the Monte Carlo method was not large enough. However, it is apparent that these two profiles are in an excellent agreement. The more photons are traced, the more accurate the transmission profile will be.

In the second experiment, we placed a source in the biological tissue and a rectangle CCD detector parallel to the generatrix of the cylinder shown as Figure 9a. The detector pitch was 20 μm . The transmission signals on the CCD detector plane from MOSE and the experiment are shown in Figure 9b and c, respectively. An excellent agreement was observed as well.

According to relative positions of the two sources and the detector plane, there were various combinations in the third

experiment. Some representative data is provided here for brevity. The parameters of the two bioluminescent sources, the biological tissue and the CCD detector plane, are given in Tables 4, 5, and 6, respectively. There are four configurations of the sources and detectors in different positions as shown in Figure 10a. The transmission profiles from MOSE and phantom experiments, respectively, shown in Figures 10b and c indicate once more that all the corresponding results are really consistent.

DISCUSSION

We emphasize that the MOSE provides significant features that are different from existing simulators. For example, compared with a typical simulation software package named "Monte Carlo Modeling of Light Transport in

Table 6
CCD Detector Parameters Used in Comparison Between MOSE and Three Phantom Studies

Experiment No.	Shape	Center (mm)	Height (mm)	Width (mm)	Each Pixel Size (μm)
1	rectangle	(0, 0, 5.2)	31.9	2	38
2	rectangle	(10.2, 0, 0)	26.8	26	20
3	rectangle	Design 1 (10.2, 0, 0) Design 2 (0, 10.2, 0) Design 3 (-10.2, 0, 0) Design 4 (0, -10.2, 0)	26.8	26	20

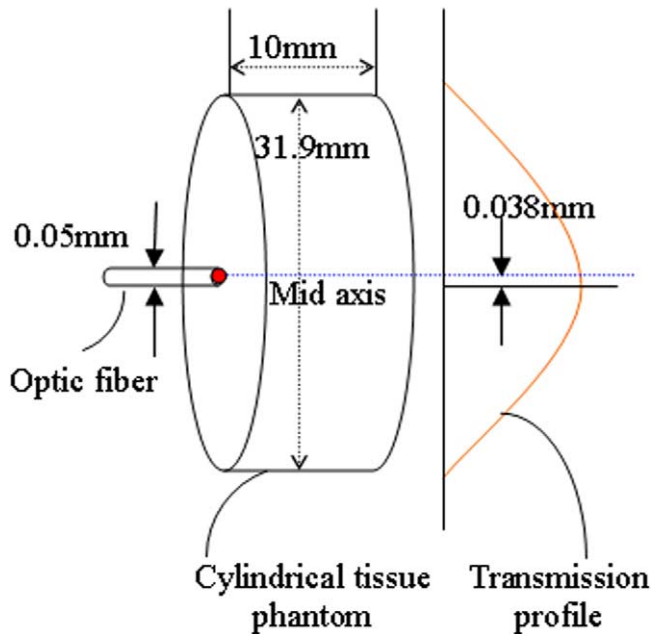


Figure 7. Experimental set-up for phantom study 1.

Multi-layered Tissues (MCML),” (6,13), the MOSE allows building blocks suitable for small animal imaging, while the MCML was designed for layered tissue structures. Compared with the TracePro (20), the MOSE is dedicated to the bioluminescent imaging of small animals. It does not carry a large amount of overhead of the TracePro but also enables a number of functions particularly valuable in our intended applications.

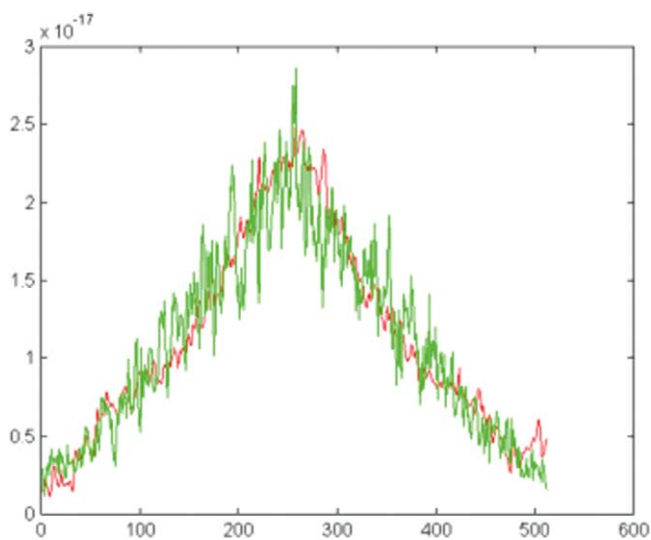


Figure 8. Comparison between MOSE and phantom study 1. The sparser and heavier curves represent the results of MOSE and phantom study 1, respectively.

As with any software package, there are a variety of aspects to improve the MOSE. Our long-term commitment is to develop a bioluminescence tomography, and we will continue refining the MOSE to make an outstanding tool in the research field. First of all, we incorporate a segmented CT/micro-CT volumes and a large optical data base into the simulator. The image volume of a mouse can be easily obtained with a CT scanner. With special software, optical properties will be assigned to each segment relying on a dedicated library that was built by measuring various tissues using literature data and an oblique-incidence reflectometer. These segmented images with optical properties are used as the input of the MOSE. Secondly, a user-friendly module with easy modification will be implemented to increase the complexity of the source model in 3D. Either surface or volume bioluminescent sources can be easily drawn and modified with simple operations (eg, moving, adding, or deleting several culminations of the source shape) upon user requirement. In addition, we will investigate the methods to fit bioluminescent signal by altering the source from all the available information. Thirdly, we will transplant the software into a PC cluster in the near future. We will split the emission spectrum (500–760 nm) into 32 consecutive segments during Monte Carlo simulations because the tissue optical properties are wavelength-dependent. Each segment will be simulated by one node of our PC cluster. We will further divide the spectrum into 64 segments or more if the segments are not fine enough to observed accuracy. It is worth mentioning that we will optimize the segment division as well. We attempt to make even distribution on the axis of optical properties for the segments rather than on the wavelength axis to minimize the spread of optical properties in each segment.

In conclusion, a Monte Carlo simulator MOSE has been developed as a mouse optical simulation environment. It is an important component of the biolumines-

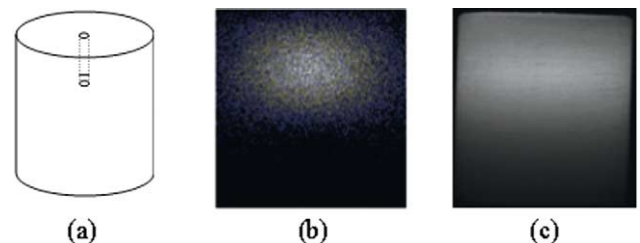


Figure 9. Experimental set-up and results of phantom study 2. Panel (a) presents the experimental set-up including one bioluminescent source and one cylindrical tissue; (b) describes the transmission profiles of MOSE; and (c) shows the transmission profiles of phantom study 2.

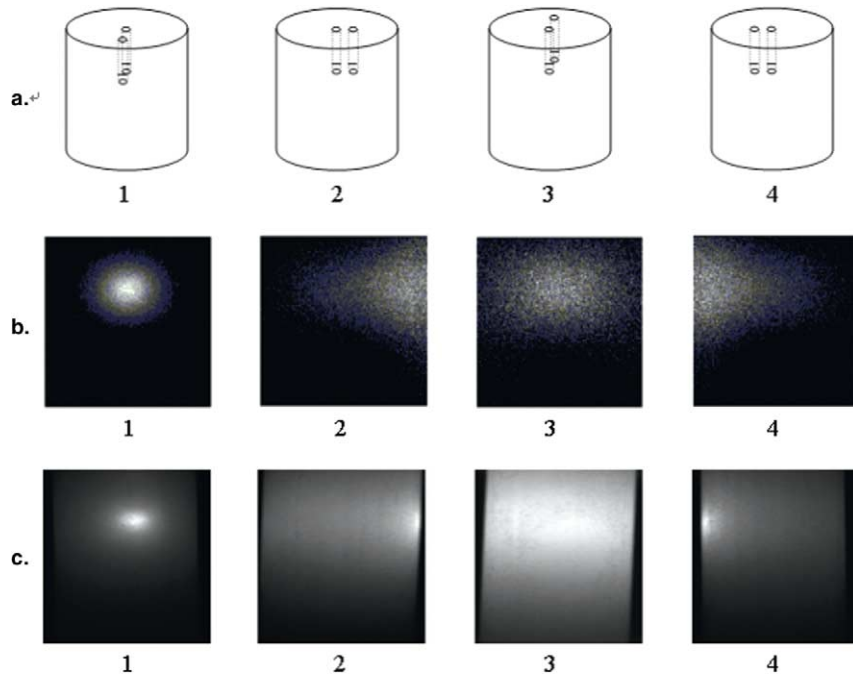


Figure 10. Experimental set-up and results of phantom study 3. **a1–a4** show four representative experimental set-up according to the relative positions between two bioluminescent sources and the cylindrical tissue. The detector plane is located at the front of the cylindrical tissue. **b1–b4** present the transmission profiles of MOSE; and **c1–c4** indicate the transmission profiles of phantom study 3.

cence tomography project. With building solids provided by the MOSE, tissue models and source models can be satisfactorily constructed for studies on bioluminescent imaging. The MOSE is accurate, flexible, and efficient for simulating the photon transport in bioluminescence tomography as shown in our work. Further improvements are ongoing to expand the utilities of the MOSE.

REFERENCES

- Weissleder R, Mahmood U. Molecular imaging. *Radiol* 2001; 219:316–333.
- Blasberg RG, Gelovani-Tjuvajev J. In vivo molecular-genetic imaging. *J Cell Biochem* 2002; 87:172–183.
- Rice BW, Cable MD, Nelson MB. In vivo imaging of light-emitting probes. *J Biomed Opt* 2001; 6:432–440.
- Wang G, Hoffman EA, McLennan G. Bioluminescent CT method and apparatus. US provisional patent application, March 2003.
- Wang G, Hoffman EA, McLennan G, et al. Development of the first bioluminescent tomography system. *Radiology* 2003;229(P):566.
- Wang LH, Jacques SL, Zheng LQ. MCML – Monte Carlo modeling of light transport in multi-layered tissues. *Comput Methods Programs Biomed* 1995; 47:131–146.
- Prahl SA, Keijzer M, Jacques SL, et al. A Monte Carlo model of light propagation in tissue. *Proc SPIE* 1989; 5:102–111.
- Prahl SA. Calculation of light distributions and optical properties of tissues. PhD Dissertation, Department of Biomedical Engineering, University of Texas at Austin, 1988.
- Kim AD, Keller JB. Light propagation in biological tissue. *J Opt Soc Am* 2003; 20:92–98.
- Flock ST, Wilson BC, Wyman DR, et al. Monte Carlo modeling of light-propagation in highly scattering tissues – I: model predictions and comparison with diffusion theory. *IEEE Trans Biomed Eng* 1989; 36:1162–1168.
- Flock ST, Wilson BC, Wyman DR, et al. Monte Carlo modeling of light-propagation in highly scattering tissues – II: comparison with measurements in phantoms. *IEEE Trans Biomed Eng* 1989; 36:1169–1173.
- Arridge SR, Schweiger M, Hiraoka M, et al. A finite element approach for modeling photon transport in tissue. *Med Phys* 1993; 20: 299–309.
- Wang LH, Jacques SL. Monte Carlo modeling of light transport in multi-layered tissues in standard C. University of Texas M. D. Anderson Cancer Center, 1992.
- Jacques SL, Wang LH. Monte Carlo modeling of light transport in tissues. In: Welch AJ, et al (eds). *Optical thermal response of laser irradiated tissue*. New York, NY: Plenum Press, 1995; 73–100.
- Lux I, Koblinger L. Monte Carlo particles transport methods: Neutron and photon calculations. Boca Raton, FL: CRC Press, 1991.
- Hecht E. *Optics*. 2nd ed. Reading, MA: Addison-Wesley, 1987.
- Henry LG, Greenstein JL. Diffuse radiation in the galaxy. *Astrophys J* 1941; 93:70–83.
- Hendricks JS, Booth TE. MCNP variance reduction overview. *Lect Notes Phys* 1985; 240:83–92.
- Cong WX, Wang LH, Wang G. Formulation of photon diffusion from spherical bioluminescent sources in an infinite homogeneous medium. *Biomed Eng Online* 2004; 4:12
- User's Manual (release 3.0) of TracePro (Software for Opto-Mechanical Modeling). Lambda Research Corporation, Littleton, MA.